2016 International Symposium on Nonlinear Theory and Its Applications,
NOLTA2016, Yugawara, Japan, November 27th-30th, 2016

Abnormal Cardiac Conduction in Acquired Heart Disease: a Simulation Study

Kunichika Tsumoto† and Yoshihisa Kurachi†

†Division of Molecular and Cellular Pharmacology, Graduate School of Medicine, Osaka University
2–2 Yamada-oka, Suita, Osaka 565-0871, Japan
Email: tsumoto@pharma2.med.osaka-u.ac.jp, ykurachi@pharma2.med.osaka-u.ac.jp

Abstract—The voltage-gated sodium (Na) channels, playing key roles in the action potential (AP) initiation and the propagation, alters the distribution within a myocyte in congenital and acquired disorder. Here, we show that the Na channel distribution at the subcellular level may be partly contributed to the conduction disorder and the initiation of reentrant tachyarrhythmia by using computer simulation. These results suggest that the function of ion channels as well as the subcellular distribution may be partly responsible for the occurrence of lethal arrhythmia.

1. Introduction

The Cardiac Arrhythmia Suppression Trial (CAST) [1, 2] showed that the risk of arrhythmia-related death was increased in patients with old myocardial infarction, although Na channel blockers like class I antiarrhythmic drugs reduced premature ventricular contractions (PVCs), which degenerate into tachyarrhythmias. However, it remains controversial whether the poor prognosis is due to the negative inotropic and/or proarrhythmic effects of Na channel blockers.

It has been theoretically confirmed that a hypothetical conduction mechanism based on the microstructure of ventricular myocytes, i.e., electric field (EF) mechanism; the electrical communication between the adjacent cells was mediated by the change in the large negative extracellular potential induced at the narrow intercellular cleft space facing the intercalated discs (IDs), i.e., junctional membranes (JMs), serves as one of the homeostatic mechanisms of excitation conduction under conditions of reduced gap junctional coupling in the diseased heart [3, 4]. Here, we extend this idea to the proarrhythmic mechanism under the conditions of 5-day infarcted canine heart of which gap junctional coupling is not reduced yet [5]. Baba et al.[6] found that the subcellular redistribution of Na channels occurs at the ischemic border zone (IBZ) of 5-day infarcted canine ventricles, leading to marked decrease of Na channel expression in the lateral membrane (LM) of cardiomyocyte. The aim of this study was to reveal the role of the subcellular Na channel redistribution in proarrhythmic effects of Na channel blockers on ventricular arrhythmias under ischemia. The combined effects of the subcellular redistribution of Na channels and the Na channel blockade on excitation conduction were investigated by altering the subcellular Na channel distribution of each myocyte in a myofiber model, and proarrhythmic effects of class I antiarrhythmic drugs on infarcted ventricular tissue were evaluated on the basis of the conduction properties in the simulated myofibers.

2. Methods

2.1. Myofiber model

We constructed a myofiber model comprising of 100 ventricular myocytes, each of which was 100 μm in length and 22 μm in diameter (Fig.1A). The myocytes were electrically connected with both gap junctions and the EF

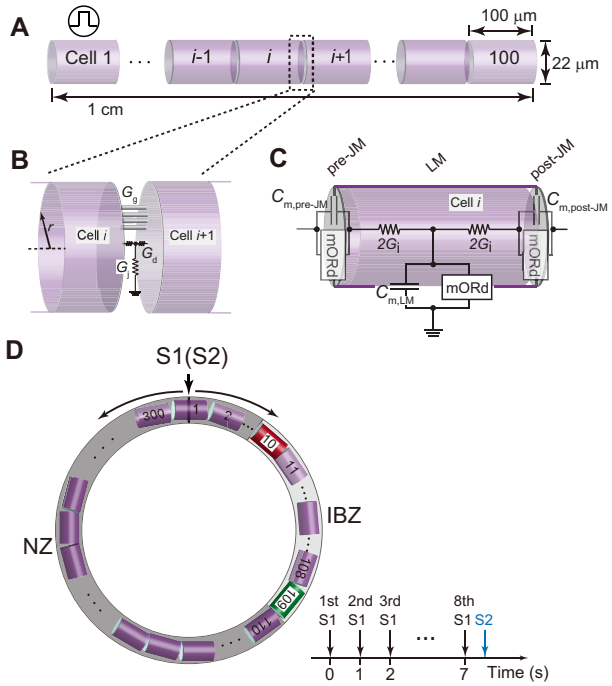

Figure 1: Myocardial fibers and rings. (A), Schematic representation of a myocardial fiber comprising cylindrical 100 cells. (B), Schematic representations of the intercellular junction. (C), The AP of each membrane segment is represented by the modified O'Hara–Rudy dynamic (mORd) human ventricular myocyte model. (D), Schematic representation of the myocardial ring comprising 300 cells (*left*), and the pacing protocol (*right*).

mechanism [3, 4] (Figs.1B). On the basis of previous experimental data [5] reporting that the intercellular gap junctional conductance (G_g) of the IBZ in 5-day infarcted canine heart did not differ significantly from that of the non-ischemic zone (NZ), we employed the same G_g in both the IBZ and NZ myofiber models: 2.534 μS. The radial cleft conductance (G_j) [3] and series axial cleft conductance (G_d) were 0.25 μS and 33.8 mS, respectively [4].

Each myocyte in the myofiber model comprised 3 segments: 2 for the JM (i.e., post- and pre-JMs), and the other one for the LM (Fig.1C). The membrane segments were represented by a modified O'Hara–Rudy dynamic (ORd) model [7, 8].

2.2. Myocardial ring model

To evaluate effects of Na channel blockade on the vulnerability of a myocardial ring model comprising an NZ and IBZ (Fig.1D, left) to PVCs, additional simulations were performed using the S1-S2 stimulation protocol: 8 S1 stimuli with a basic cycle length of 1,000 ms were applied transmembranously followed by an S2 stimulus with various coupling intervals (Fig.1D, right). There were 100 (cells 11–110) and 200 (cells 111–10) cells in the IBZ and NZ, respectively.

2.3. Subcellular Na channel distribution

The Na channel conductance was 14.868 nS/pF [8]. Thus, the entire Na channel conductance of each myocyte corresponded to 1.14 μS (G_{Na}), which was defined as the control value. We altered the subcellular distribution of Na channels by allocating the entire Na channel conductance to each membrane segment. The Na channel conductances of the JM and LM were expressed as percentages of the G_{Na}: $\%g_{\mathrm{Na,JM}}$ and $\%g_{\mathrm{Na,LM}}$, respectively. Thus, the entire Na channel conductance ($\%g_{\mathrm{Na,JM+LM}}$) was equal to the sum of $\%g_{\mathrm{Na,JM}}$ and $\%g_{\mathrm{Na,LM}}$.

As the Na channel current amplitude at the LM becomes about the same as that of IDs [9], we determined the subcellular Na channel distribution in the NZ. In particular, the Na channel conductance in the JM and LM of a myocyte located in the NZ were estimated to be half of the entire Na channel conductance [9].

2.4. Na channel blockade

Na channel blockade by the administration of class I antiarrhythmic drugs was achieved by reducing the entire Na channel conductance while maintaining the ratio of $\%g_{\mathrm{Na,JM}}$ to $\%g_{\mathrm{Na,LM}}$. The ratio of Na channel blockade was expressed as a percentage of the G_{Na} ($\%G_{\mathrm{Na}}$ block).

2.5. Computations

Numerical calculations were performed as described previously [4]. Pacing stimuli of twice the diastolic threshold were applied to the LM segment of a myocyte located at one end of the myofiber.

3. Results

3.1. Na channel blockade and conduction velocity

Figure 2A shows the relative ratios of conduction velocity (CV) normalized by CV in the myocardial fiber with $50\%g_{\mathrm{Na,JM}}$ and $50\%g_{\mathrm{Na,LM}}$, i.e., the subcellular Na channel distribution in the NZ, as a function of $\%g_{\mathrm{Na,JM+LM}}$ in each myocyte of the myofiber model. Thus, the CV under NZ myofiber condition were 52.6 cm/s. In the case of $\%g_{\mathrm{Na,JM}}$ change (Fig.2A, open squares with solid line), the %CV decreased not more than 10%

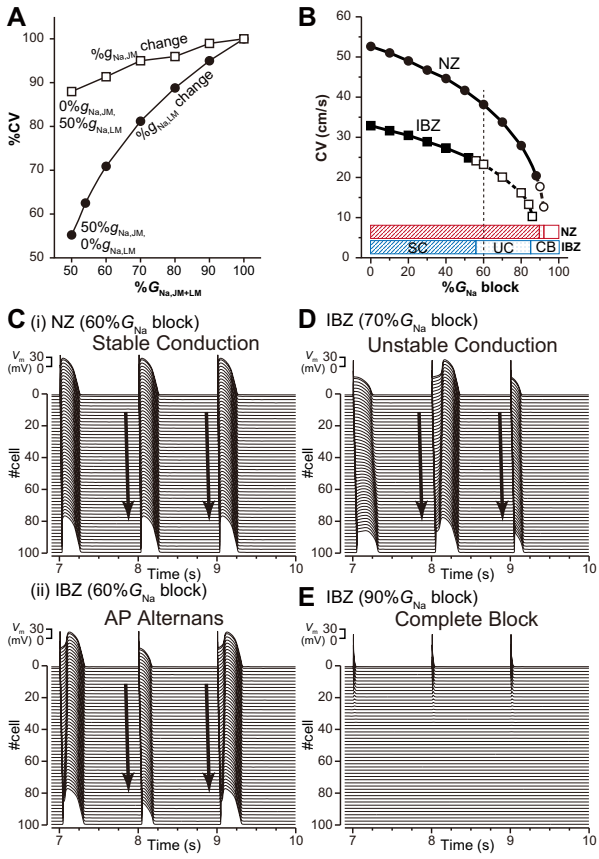

Figure 2: Effects of subcellular Na channel distribution on CV and destabilization of AP propagation by Na channel blockade. (A), Relative ratios of conduction velocity (%CV) as a function of $\%g_{\mathrm{Na,JM}}$ or $\%g_{\mathrm{Na,LM}}$ in each myocyte of the myofiber model. (B), CV as a function of $\%G_{\mathrm{Na}}$ block. The relationship between the AP propagation patterns and $\%G_{\mathrm{Na}}$ block is represented by the bottom bars. SC, stable conduction; UC, unstable conduction (e.g., AP alternans); CB, complete conduction block. (C)–(E), Examples of AP propagation observed in NZ and IBZ myofibers.

as the $\%g_{Na,JM}$ was reduced under the condition with $50\%g_{Na,LM}$. Meanwhile, in the case of $\%g_{Na,LM}$ change (Fig.2A, filled circles with solid line), the %CV decreased markedly as a function of $\%g_{Na,LM}$ decrease under the condition with $50\%g_{Na,JM}$. On the basis of the experimentally measured CV [10] with reference to the previous immunostaining data [6], we determined the subcellular Na channel distribution in the IBZ as $50\%g_{Na,JM}$ and $4\%g_{Na,LM}$; the CV in the IBZ myofiber model was 32.9 cm/s.

Figure 2B shows CV as a function of $\%G_{Na}$ block. In both NZ and IBZ myofibers, CVs decreased gradually with $\%G_{Na}$ block. Figure 2C shows typical examples of the AP propagation observed in NZ and IBZ myofibers with $60\%G_{Na}$ block. The AP of each myocyte in the NZ myofiber with $60\%G_{Na}$ block was able to propagate through the myofiber (Fig.2C(i)), whereas the same $60\%G_{Na}$ block in the IBZ myofiber caused AP alternans (Fig.2C(ii)). The critical values of the $\%G_{Na}$ block maintaining stable conduction were 88% and 54% in the NZ and IBZ myofibers, respectively (Fig.2B, bottom, red and blue bars denoted by SC, respectively). $\%G_{Na}$ block increases exceeding the critical value in both NZ and IBZ myofibers caused unstable conduction. Typical examples of unstable conduction observed in the IBZ myofiber are shown in Fig.2D. The further increase in $\%G_{Na}$ block caused complete conduction block (Fig.2E). In the NZ myofiber, the AP did not propagate when the entire Na channel conductance within the myocyte was reduced by 94%. Complete conduction block in the IBZ myofiber occurred with $88\%G_{Na}$ block.

3.2. Reentry induction in a myocardial ring model

A phase diagram of the excitation conduction in response to S1–S2 interval for a given degree of Na channel blockade is shown in Fig.3A. Open circles labeled *a–d* in Fig.3A correspond to Figs.3B(a)–(d), respectively. The blue region in Fig.3A represents the failure of AP induction due to the refractory period at the S2 stimulus site (Fig.3B(a)). Meanwhile, the gray region in Fig.3A denotes the bidirectional conduction from the S2 stimulus site, resulting in the collision of excitation waves (Fig.3B(b), asterisk). The red region in Fig.3A represents the conditions of reentry (i.e., counterclockwise rotation) induction shown in Fig.3B(c). The green region in Fig.3A (i.e., further increase in the $\%G_{Na}$ block) denotes the conduction block occurring at both the proximal and distal borders of the IBZ (Fig.3B(d)). In contrast, in the case of $80\%G_{Na}$ block in the control model without an IBZ, no the S1-S2 intervals initiating reentry was observed.

4. Discussion

4.1. Major findings

The major findings of the present study are as follows:(1) a decrease in Na channels from the LM of each ventricular myocyte was a major cause of the conduction slowing

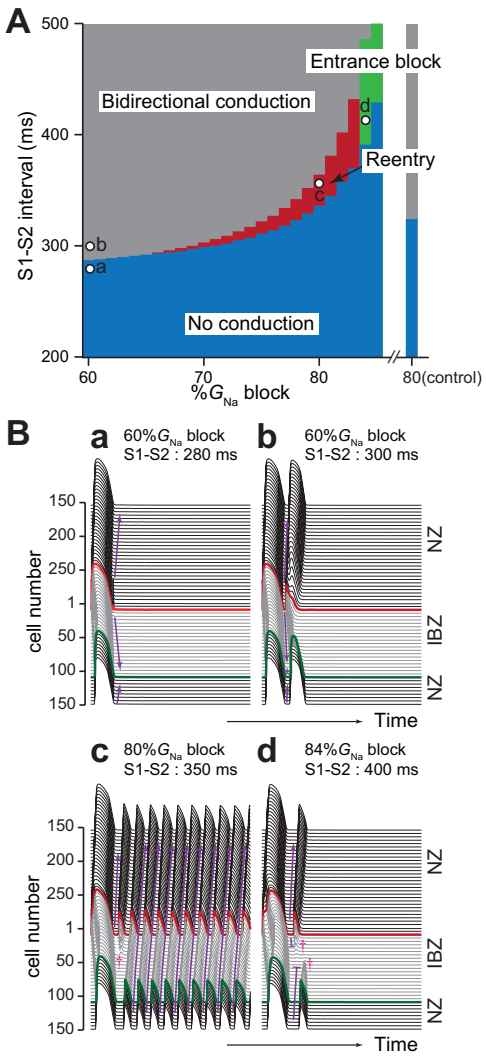

Figure 3: Reentry induction by Na channel blockade in myocardial ring models. (A), Phase diagram of $\%G_{Na}$ block vs. S1–S2 interval showing proarrhythmic events under Na channel blockade in the myocardial ring model. Right bar (control): responses to S2 stimulus in the myocardial ring constructed of only NZ myocytes under $80\%G_{Na}$ block. (B), Examples of AP propagation in response to S1–S2 interval. Arrows and purple short bars indicate the directions of AP propagation and entrance block, respectively.

in the IBZ; (2) an IBZ with the subcellular redistribution of Na channels was highly vulnerable to reentry under Na channel blockade. These findings suggest that the subcellular Na channel redistribution in the IBZ leads to decreased tissue excitability and that such a phenomenon is facilitated by Na channel blockers. Na channel blockade tended to cause a unidirectional conduction block toward the IBZ, resulting in the induction of reentrant tachyarrhythmia following PVC. Thus, the proarrhythmic effects of Na channel

blockers in patients with old myocardial infarction might be partly attributed to the ischemia-related subcellular redistribution of Na channels.

4.2. Proarrhythmic effects of Na channel blockade under ischemia

Cabo et al. found that the CV in the IBZ of 5-day infarcted canine ventricles is 36% slower than that in the NZ (29 vs. 45 cm/s, respectively)[10]. The experimentally observed conduction slowing in the IBZ [10] may be attributable to the subcellular Na channel redistribution via EF mechanism, because not a decrease in Na channels from the JM but the LM within each myocyte in the myofiber model resulted in a similar decrease in CV (37.5%; Fig.2A, filled circles with solid line).

Excitation conduction was more easily blocked by Na channel blockade in the IBZ than the NZ because of the marked decrease in the excitability of IBZ (Fig.2B). Accordingly, we speculate that subcellular Na channel redistribution together with Na channel blockade causes a unidirectional block at sites near the IBZ. Indeed, Na channel blockade with the coexistence of an NZ and IBZ widened the vulnerable period for PVCs (Fig.3A, red region) compared to the cases with $\leq 65\% G_{\mathrm{Na}}$ block. Furthermore, unidirectional block induced by a stimulus applied at a site near the IBZ initiated reentry (Fig.3B(c)).

On the other hand, as shown in Fig.2B, there existed a range of Na channel blockade causing unstable conductions (Figs.2C(ii) and D) between the ranges of stable conduction (Fig.2C(i)) and conduction block (Fig.2E). Such unstable conductions might be involved in arrhythmogenic mechanisms under ischemia [11]. Baba et al. have reported that the subcellular Na channel redistribution occurred heterogeneously at the IBZ [6]. Therefore, heterogeneous Na channel blockade in the IBZ might also cause an unstable conduction. Taken together, the present results suggest that even if the number of PVCs is reduced as a result of the continuous administration of class I antiarrhythmic drugs, the subcellular Na channel redistribution under Na channel blockade increases the ventricular vulnerability to PVCs, leading to the initiation of reentrant tachyarrhythmias and consequently more arrhythmic events [1, 2].

Acknowledgments

This work was supported by grants from JSPS KAKENHI Grant Numbers 24790214 and The Takeda Science Foundation to KT, and MEXT KAKENHI Grant Numbers 22136002 to YK.

References

[1] The Cardiac Arrhythmia Suppression Trial (CAST) Investigators, "Preliminary report: effect of encainide and flecainide on mortality in a randomized trial of arrhythmia suppression after myocardial infarction," *N. Engl. J. Med.*, vol.321, pp.406–412, 1989.

[2] D. S. Echt, P. R. Liebson, L. B. Mitchell, R. W. Peters, D. Obias-Manno, et al., ' 'Mortality and morbidity in patients receiving encainide, flecainide, or placebo. The Cardiac Arrhythmia Suppression Trial," *N. Engl. J. Med.*, vol.324, pp.781–788, 1991.

[3] N. Sperelakis, J. E. Mann Jr, "Evaluation of electric field changes in the cleft between excitable cells," *J. Theor. Biol*, vol.64, pp.71–96, 1977.

[4] K. Tsumoto, T. Ashihara, R. Haraguchi, K. Nakazawa, Y. Kurachi, "Roles of subcellular Na^+ channel distributions in the mechanism of cardiac conduction," *Biophys. J*, vol.100, pp.554–563, 2010.

[5] J. A. Yao, W. Hussain, P. Patel, N. S. Peters, P. A. Boyden, et al., "Remodeling of gap junctional channel function in epicardial border zone of healing canine infarcts," *Circ. Res*, vol.92, pp.437–443, 2003.

[6] S. Baba, W. Dun, C. Cabo, P. A. Boyden, "Remodeling in cells from different regions of the reentrant circuit during ventricular tachycardia," *Circulation*, vol.112, pp.2386–2396, 2005.

[7] T. O'Hara, L. Virág, A. Varró, Y. Rudy, "Simulation of the undiseased human cardiac ventricular action potential: model formulation and experimental validation," *PLoS. Comput. Biol*, vol.7, e1002061, 2011.

[8] K. Tsumoto, Y Kurachi, "A novel conduction mechanism linking cardiac action potentials and excitation propagation: electric field mechanism," *Trans. of JSMBE*, vol.53, pp.138–143, 2015. (in japanese)

[9] A. O. Verkerk, A. C. van Ginneken, T. A. van Veen, H. L. Tan, "Effects of heart failure on brain-type Na^+ channels in rabbit ventricular myocytes," *Europace*, vol.9, pp.571–577, 2007.

[10] C. Cabo, J. Yao, P. A. Boyden, S. Chen, W. Hussain, et al., "Heterogeneous gap junction remodeling in reentrant circuits in the epicardial border zone of the healing canine infarct," *Cardiovasc. Res*, vol.72, pp.241–249, 2006.

[11] J. Coromilas, C. Costeas, B. Deruyter, S. M. Dillon, N. S. Peters, et al. "Effects of pinacidil on electrophysiological properties of epicardial border zone of healing canine infarcts: possible effects of KATP channel activation," *Circulation*, vol.105, pp.2309–2317, 2002.